PROPERTIES OF EAS GONIOMETER TEL

All definitions of the values and functions used see in the part «GONIOMETER'S GENERIC PROPERTIES»

The TEL goniometer is operating now

J. Gogebashvili Telavi State University, Telavi, Georgia

Location of the TEL installation

Latitude	41.910317°N
Longitude	45.468339°E
Altitude	$(845 \pm 4)\ m$ above sea level
Upright atmospheric mass depth	$X^{\uparrow}_{\mathrm{TEL}} = 936.4\ g/cm^2$
Air density at this location	$\rho_{\mathrm{TEL}} = 1129\ g/m^3$
and the corresponding multiple scattering unit	$rM_{\mathrm{TEL}} = 85.2m$

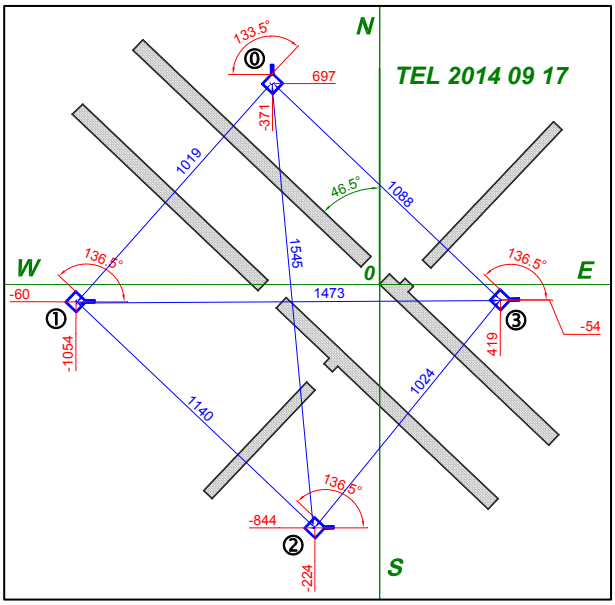

Figure 1 TEL array layout.
All linear dimensions are measured in centimeters.

The "flat" detectors of TEL goniometer are located under the concrete roof of first building of J. Gogebashvili Telavi State University in Telavi, Georgia. The mass depth of this filter is accepted to be $X_{\mathrm{filter}} = 30.8\ g/cm^2$ for all directions and the radiation length for the actual absorber's substance is accepted to be $T_{\mathrm{filter}} = 27.5\ g/cm^2$

Number of detectors $N = 4;\quad d = 0,1,2,3$

The areas of all plastic scintillator slabs are $S_d = 0.25m^2;\quad \{SS_{\mathrm{TEL}}\} = (S_0, S_1, S_2, S_3,)$

The detectors' positions layout in the roof space is shown in the **figure 1**.

Local $(E, N)^{\mathrm{T}}$ coordinates of the detectors are obtained by two-dimensional multilateration procedure relative to the fixed points on the circumscribing walling with subsequent rotation by 46.5° about the vertical axis:

$$\{\mathbf{rr}_{\mathrm{TEL}}\} = \begin{pmatrix} -371 & -1054 & -224 & 419 \\ 697 & -60 & -844 & -54 \end{pmatrix} cm \quad \begin{matrix} "E" \\ "N" \end{matrix}$$

The practically occurred EAS observation rate at TEL goniometer's performance during the 2020 year observation session is

$$ExpRate_{\mathrm{TEL}} = (24.49 \pm 0.84)\ hr^{-1}.$$

The required effective common threshold of sensitivity n^*_{TEL} of all detectors used is estimated by numerical solving of the equation

$$\widetilde{\mathrm{Rate}}(n^*_{\mathrm{TEL}}) = ExpRate_{\mathrm{TEL}}$$

shown in the **figure 2**. Here $\widetilde{\mathrm{Rate}}(n^*)$ is the interpolation polynomial curved upon the set of calculated rates for the series of arbitrarily assigned values n^* of supposed thresholds of sensitivity. The effective common threshold of sensitivity of all detectors is estimated as $n^*_{\mathrm{TEL}} = 2.6279$ particles per detector

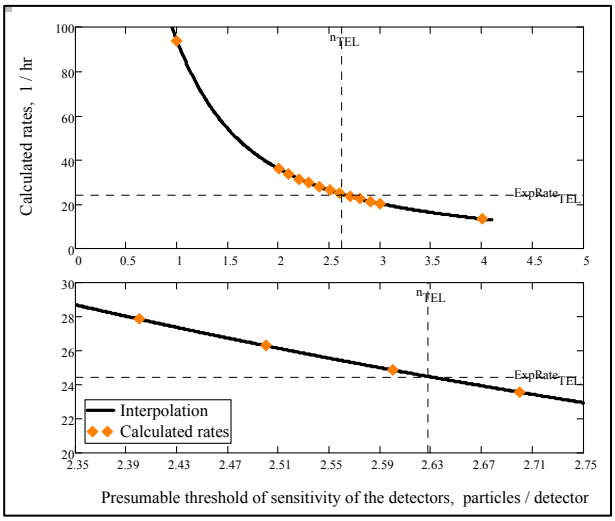

Figure 2 1Plot of the numerical estimation of the effective common threshold of sensitivity of the detectors of TEL goniometer.

Therefore the aggregate variable TEL describing the native properties of the TEL goniometer is established as $TEL = \left[X^{\uparrow}_{\mathrm{TEL}}, \{\mathbf{rr}_{\mathrm{TEL}}\}, \{SS_{\mathrm{TEL}}\}, \{nn^*_{\mathrm{TEL}}\}\right]$. Every consequent calculation uses this set of properties.

The properties evaluated

The calculated rate of EAS observations by TEL goniometer is $Rate_{\mathrm{TEL}} = 24.47\ hr^{-1}$ while the observations rate is $ExpRate_{\mathrm{TEL}} = (24.49 \pm 0.84)\ hr^{-1}$.

The aperture function of the TEL goniometer

The estimated dependence of the TEL goniometer's aperture ${}^{(TEL)}\mathrm{Ap}(E)$ on the showers' energy E is shown in the **figure 3**.

The lower energy threshold of the observable EAS events is

$${}^{(TEL)}E_{\mathrm{thr}} = 2.3\times10^{5}\ GeV = 2.3\times10^{14}\ eV$$

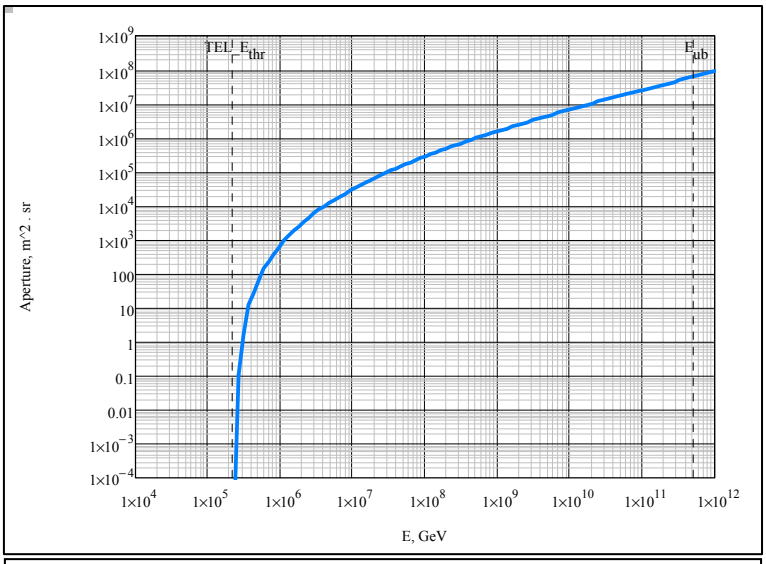

Figure 3. Dependence of the TEL goniometer's aperture on the showers' energy E

The probability density function of the EAS energies observable by the TEL goniometer

The estimated density function of the EAS energies E observable by the TEL goniometer ${}^{(TEL)}\mathrm{f_E}(E)$ is shown in the **figure 4**.

The average energy of the observable showers is

$$ {}^{(TEL)}E_{\mathrm{av}} = 9.6\times10^{6}\ GeV $$
$$ = 9.6\times10^{15}\ eV $$

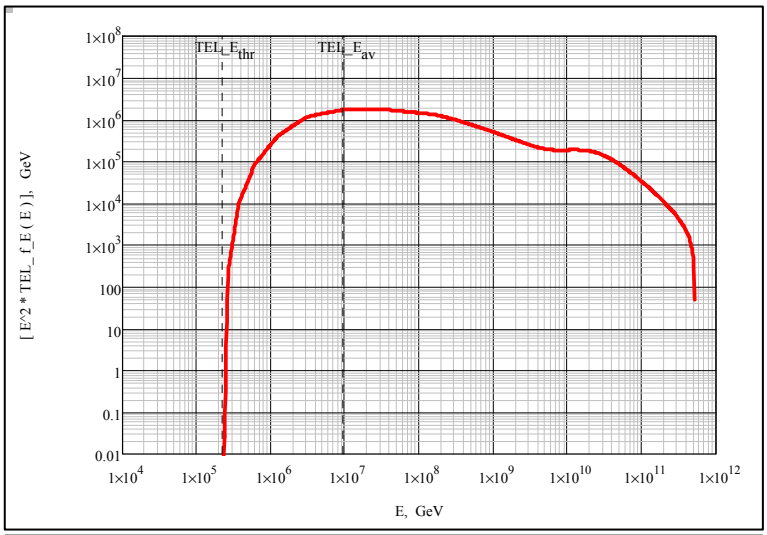

Figure 4. The EAS energy E distribution density for TEL goniometer observations is shown. Density values are scaled by corresponding energy E in the power 2.0

The integral distribution function of the EAS energies observable by the TEL goniometer

The estimated total number of EAS events observable by TEL goniometer in the course of 1 year ${}^{(TEL)}F_{\mathrm{E}}(E_{\mathrm{min}})$ dependent on the minimal energy E_{min} of the showers' sampling part is shown in the **figure 5**.

Total rate of all showers observation is

$$ {}^{(TEL)}Rate_{\mathrm{tot}} = 214460\ EAS/year $$
$$ = 24.47\ EAS/hr $$

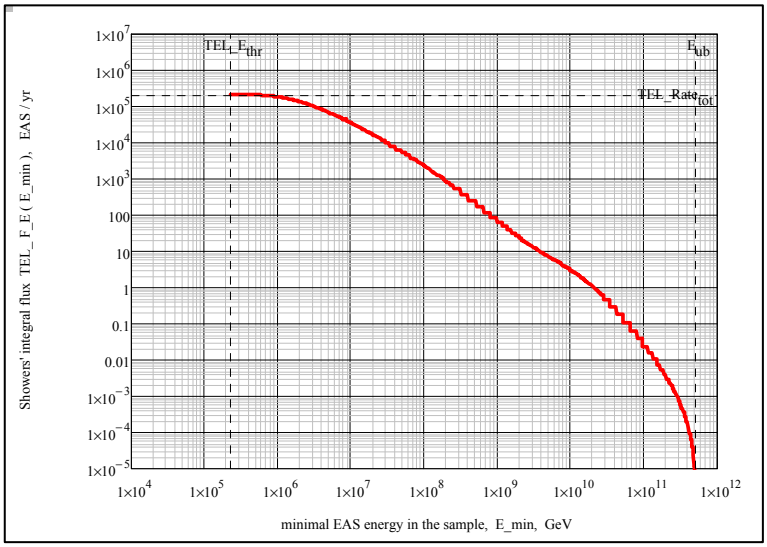

Figure 5. The curve shows the dependence on the sample minimal energy of total number of EAS events observable by TEL goniometer in the course of 1 year

The greatest accessible distance to the shower cores

The function ${}^{(TEL)}\mathrm{R}_{\max}(E)$ of the greatest accessible distance to the shower cores is defined numerically at given energy. This function is shown in the **figure 6**.

This dependence is defined in the energy interval

$${}^{(TEL)}E_{\mathrm{thr}} < E < E_{\mathrm{ub}}.$$

The maximal available distance is defined at upper bound of observable EAS energy

$$E_{\mathrm{ub}} = 516\,EeV = 5.16\times10^{20}\,eV$$

$${}^{(TEL)}maxR = {}^{(TEL)}\mathrm{R}_{\max}(E_{\mathrm{ub}}) = 3085\,m$$

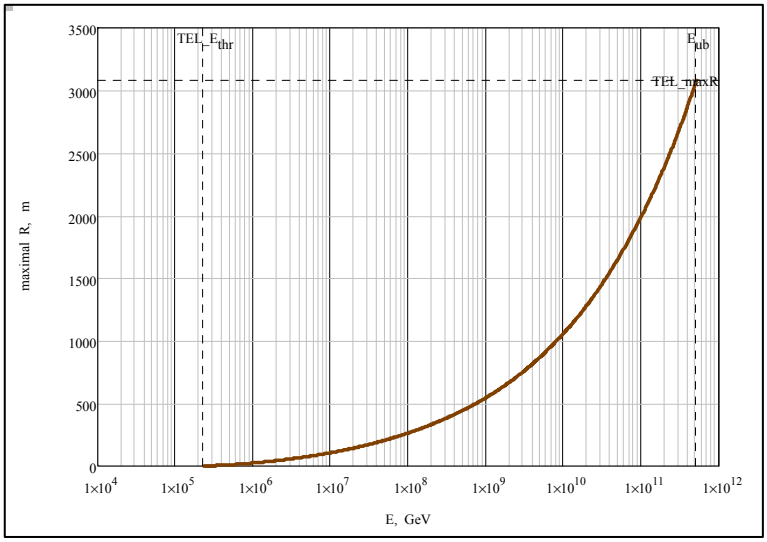

Figure 6. The energy dependence of the maximal distance from the TEL center to the EAS core intersection with the XY plane

The probability density function of the distances between the coordinate system origin and the EAS cores' points of intersection with the XY plane for the showers observable by the TEL goniometer

The probability density function ${}^{(TEL)}\mathrm{f}_{\mathrm{R}}(R)$ of the distances R to the cores of observable showers at AIP goniometer is shown in the **figure 7**.

This distribution is defined in the available distances interval

$$0 < R < {}^{(TEL)}maxR$$

$${}^{(TEL)}maxR = 3085m$$

The distance of most probable EAS observations is

$${}^{(TEL)}R_{\mathrm{mode}} = 41.0m$$

The average distance is

$${}^{(TEL)}R_{\mathrm{av}} = {}^{(TEL)}\langle R\rangle = 116.6m$$

The root mean square distance is

$${}^{(TEL)}R_{\mathrm{rms}} = \sqrt{{}^{(TEL)}\langle R^2\rangle} = 164.4m$$

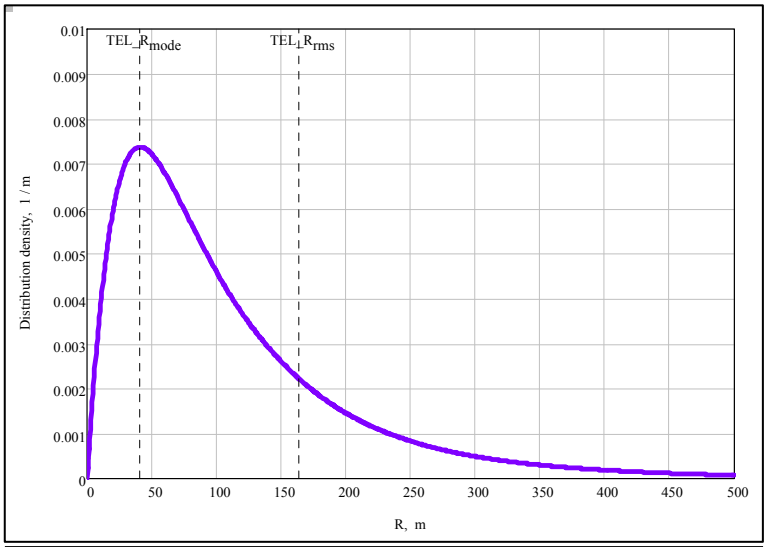

Figure 7. The distribution density of the EAS core distances R from the TEL goniometer center.

Two-dimensional distribution of the EAS core position points' observable by TEL goniometer

The diametrical section of two-dimensional distribution ${}^{(TEL)}\mathrm{f}^{(2)}(x,y)$ of the EAS core position points' observable by TEL goniometer is shown in the **figure 8**.

The average position of all EAS cores' intersections with XY plane is obviously in the goniometer's center $(x=0, y=0)$ and the standard deviation in each of (x,y) dimensions is equal to ${}^{(TEL)}\sigma R = \sqrt{{}^{(TEL)}\langle R^2 \rangle / 2} = 116.2\,m$.

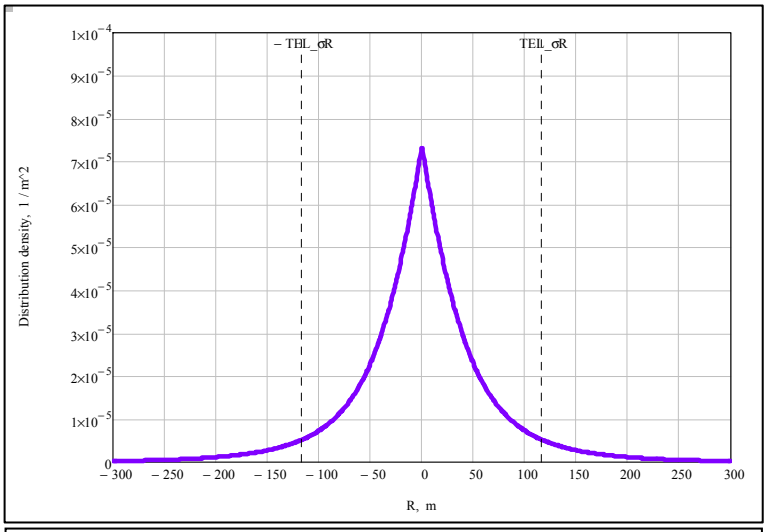

Figure 8. The diametrical section of the EAS core position points' distribution for the TEL goniometer observations.

Probability of the EAS core observation by the TEL goniometer at the distance less then *R*

The last probability is shown in the **figure 9**.

$${}^{(TEL)}\mathrm{F_R}(R) = \int_0^R {}^{(TEL)}\mathrm{f_R}(R')\,dR'$$

Approximately one-half fraction of the total number of EAS cores observable by the TEL goniometer are intersecting the XY plane within the distance of 84*m*, while the 90% part intersects within the 240*m* radius.

$${}^{(TEL)}\mathrm{F_R}\left({}^{(TEL)}R_{\mathrm{mode}}\right) = 21.6\%$$
$${}^{(TEL)}R_{\mathrm{mode}} = 41.0\,m$$

$${}^{(TEL)}\mathrm{F_R}\left({}^{(TEL)}\sigma R\right) = 64.8\%$$
$${}^{(TEL)}\sigma R = 116.2\,m$$

$${}^{(TEL)}\mathrm{F_R}\left({}^{(TEL)}R_{\mathrm{av}}\right) = 64.9\%$$
$${}^{(TEL)}R_{\mathrm{av}} = 116.6\,m$$

$${}^{(TEL)}\mathrm{F_R}\left({}^{(TEL)}R_{\mathrm{rms}}\right) = 78.9\%$$
$${}^{(TEL)}R_{\mathrm{rms}} = 164.4\,m$$

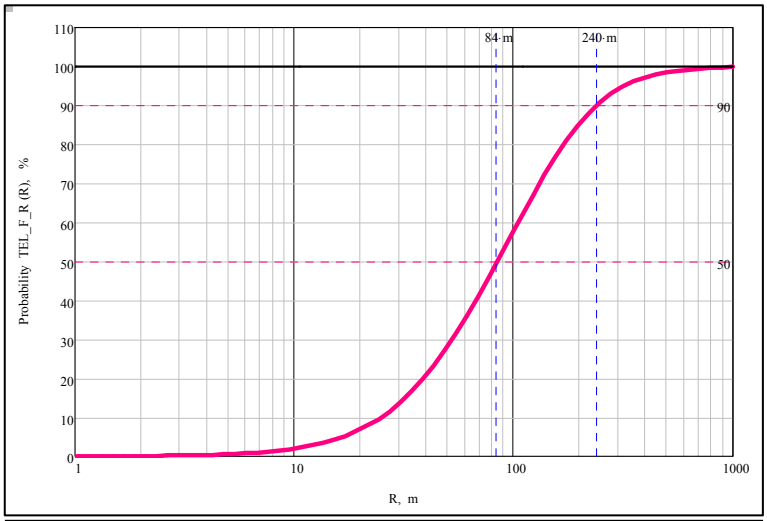

Figure 9. Probability of the EAS core observation by the TEL goniometer at the distance less then R

Borders of the areas of the observable vertical EAS cores' penetration for the TEL goniometer

Those borders are shown in the **figures 10** and **11** for some maximal EAS energies.

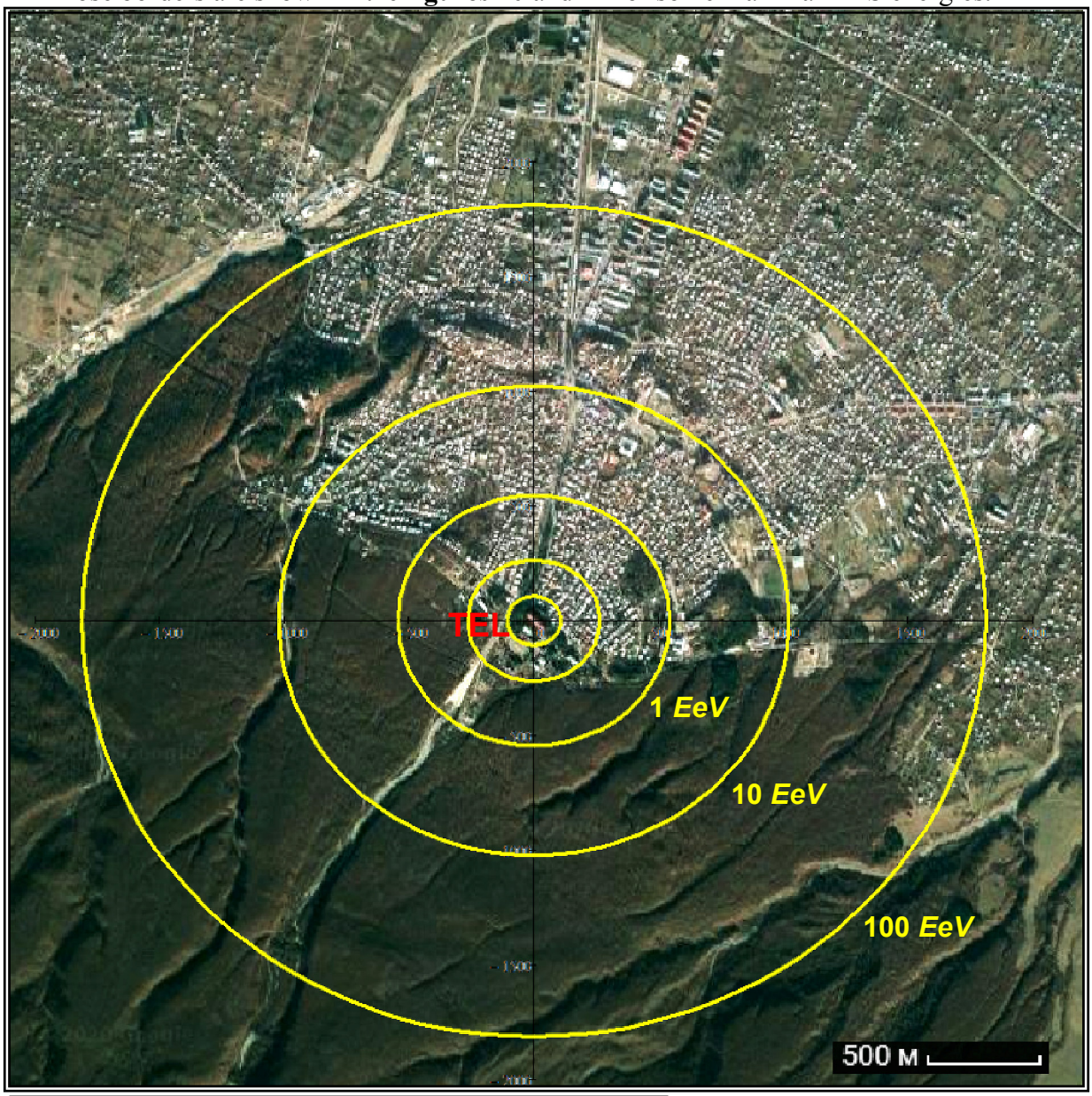

Figure 10 Borders of the areas of the TEL-observable vertical EAS cores' passage for the specified maximal total energies of the showers: 10*PeV*, 100*PeV*, 1*EeV*, 10*EeV*, 100*EeV*

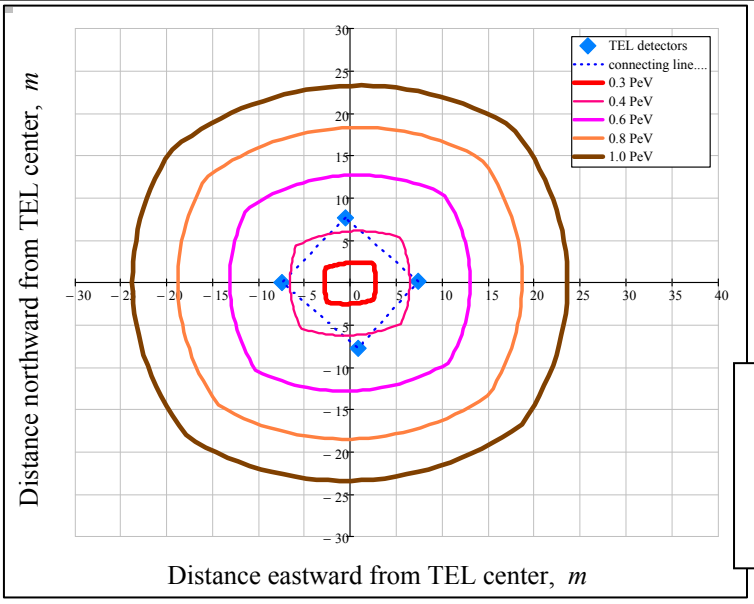

Figure 11 Borders in the TEL vicinity of the areas of the observable vertical EAS cores' passage for the maximal total energies of the showers specified in the legend